ANL/ESD/TM-87

Removal of Nitrogen Oxides from a Gas Stream by Using Monatomic Nitrogen Induced by a Pulsed Arc

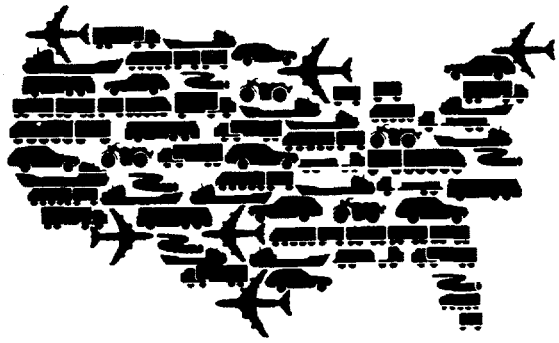

Center for Transportation Research

Argonne National Laboratory

Operated by The University of Chicago,
under Contract W-31-109-Eng-38, for the

United States Department of Energy

Argonne National Laboratory

Argonne National Laboratory, with facilities in the states of Illinois and Idaho, is owned by the United States Government, and operated by the University of Chicago under the provisions of a contract with the Department of Energy.

This technical memo is a product of Argonne's Energy Systems (ES) Division. For information on the division's scientific and engineering activities, contact:

Director, Energy Systems Division
Argonne National Laboratory
Argonne, Illinois 60439-4815
Telephone (708) 252-3724

Presented in this technical memo are preliminary results of ongoing work or work that is more limited in scope and depth than that described in formal reports issued by the ES Division.

Publishing support services were provided by Argonne's Information and Publishing Division.

Disclaimer

ANL/ESD/TM-87

Removal of Nitrogen Oxides from a Gas Stream by Using Monatomic Nitrogen Induced by a Pulsed Arc

by H.K. Ng, V.J. Novick,* K.A. Pierucci,* M.F. Geise,* and R.R. Sekar

Center for Transportation Research, Energy Systems Division,
Argonne National Laboratory, 9700 South Cass Avenue, Argonne, Illinois 60439

January 1995

Work sponsored by United States Department of Energy, Argonne National Laboratory

*Novick is affiliated with Argonne's Technology Development Division; Pierucci with the Illinois Institute of Technology, Chicago, Illinois; and Geise with the University of Notre Dame, Notre Dame, Indiana.

This report is printed on recycled paper.

CONTENTS

ACKNOWLEDGMENTS v

ABSTRACT 1

1 INTRODUCTION AND BACKGROUND 1

1.1 Sources of Nitrogen Oxides 1
1.2 Existing Emission Reduction Methods 2
1.3 Monotomic Nitrogen Method 3

2 EXPERIMENTAL APPARATUS AND PROCEDURE 5

2.1 High-Voltage Pulser System and Reaction Chamber 5
2.2 NO/NO_X and Oxygen Analyzers and Data Acquisition 5
2.3 Experimental Procedure 8

3 RESULTS 9

3.1 Experiments with NO 9
3.2 Experiments with NO_2 and NO/NO_2 Mixtures 15
3.3 Oxygen Tests 17

4 CONCLUSIONS AND RECOMMENDATIONS 25

5 REFERENCES 26

APPENDIX: Data 27

FIGURES

2.1 Schematic Design of Laboratory Layout Used for NO_x Reduction Experiment 6

2.2 Arc Reaction Area Closeup 7

3.1 NO and NO_x Reduction Efficiency vs. Power 10

3.2 NO Reduction Efficiency vs. Needle Flow Rate 11

3.3 NO_x Reduction Efficiency vs. Flow Diameter 12

3.4 NO Reduction Efficiency vs. Flow Diameter 13

3.5 Reduction Efficiency by Arc/Glass Contact Compared to Efficiency at Larger Glass Tube Diameter 14

FIGURES (Cont.)

3.6 Velocity vs. NO and NO_x Reduction Efficiency 15

3.7 Reduction Efficiency vs. NO Gas Concentration 16

3.8 NO_x Concentration vs. Power 18

3.9 NO Reduction Efficiency vs. Flow Rate 19

3.10 NO_2 Reduction Efficiency vs. Flow Rate 20

3.11 NO_2 Reduction Efficiency vs. NO_2 Gas Concentration 21

3.12 Reduction Efficiency vs. Power for Different NO-to-NO_2 Ratios 22

3.13 Percent Reduction of NO/NO_x vs. Percent Oxygen Present in the Gas Stream 23

3.14 Reduction vs. Oxygen with O_2 Flow in the Needle or in the Exhaust 24

ACKNOWLEDGMENTS

This project was supported by Laboratory-Directed Research and Development (LDRD) funds. The authors would like to thank the management of Argonne National Laboratory for allocating the discretionary funds to conduct this research. The authors are especially grateful to Larry Johnson for his guidance and inspiration. Thanks are also due to the many colleagues at the Laboratory who provided assistance with test equipment, review of results, and general support.

REMOVAL OF NITROGEN OXIDES FROM A GAS STREAM BY USING MONATOMIC NITROGEN INDUCED BY A PULSED ARC

by

H.K. Ng, V.J. Novick, K.A. Pierucci, M.F. Geise, and R.R. Sekar

ABSTRACT

The effectiveness of monatomic nitrogen, induced by a pulsed electric arc, in reducing nitric oxide (NO) and nitrogen dioxide (NO_2) was studied. The goal for this research is the reduction of nitrogen oxides (NO_x) from automobile emissions by this alternative technique, which can be cost-effective and has the potential to reduce NO_x in exhaust containing up to 10% oxygen. The initial tests with 100, 500, and 1,000 ppm NO in pure nitrogen have shown that a greater than 50% reduction of NO/NO_x is readily achievable. At an NO concentration of 100 ppm, a greater than 90% NO/NO_x reduction was recorded. Different flow rates of the monatomic nitrogen and the gas stream were tested. The flow rate of the monatomic nitrogen did not have a significant effect on the reduction efficiency, unlike the flow rate of the gas stream. The cross-sectional flow area of the gas stream was varied in order to assess whether the proximity of the gas stream to the arc would affect NO/NO_x reduction. Results of the tests revealed that the smallest cross-sectional area had the best reduction, but also the highest chance of contacting the arc. The composition of the gas stream was also varied to elucidate the effects of NO_2 and O_2 on the NO/NO_x reduction efficiency. When NO_2 and O_2 are present in the gas stream, both gases lower the reduction efficiency significantly by creating more NO or NO_2. Experiments are continuing to improve the reduction efficiency. The electrical power, a function of pulse frequency, voltage, and current, was treated as a key parameter in the investigation. The power consumption of the high-voltage pulser apparatus for a 100-kW engine was estimated to be 3 kW.

1 INTRODUCTION AND BACKGROUND

1.1 SOURCES OF NITROGEN OXIDES

Nitrogen oxides (NO_x) are produced from both natural and anthropogenic (man-made sources). A large amount of NO_x is produced from volcanic eruptions, lightning, and bacterial action in the soil. However, because naturally occurring NO_x emissions are distributed over

the entire globe, resulting air concentrations are small compared to local anthropogenic sources.[1]

The major source of NO_x emissions created by human activities is combustion of fossil fuels. NO_x is formed in two ways during combustion. Thermal NO_x is formed by the reaction of nitrogen with oxygen at high temperatures, while fuel NO_x is produced by the reaction of nitrogen that is chemically bound in the fuel with oxygen in the combustion air.[2-4]

NO_x sources include both mobile and stationary emissions; each accounts for nearly 50% of the NO_x produced by human activity in the United States.[4] Mobile emissions from vehicle exhaust are considered a greater health concern than stationary emissions, because they occur at ground level.

Because of the increasing use of automobiles, greater demand is being placed on the auto industry by the U.S. Environmental Protection Agency (EPA) to reduce vehicle emissions. Federal NO_x emissions standards were set at 1.0 g/mi at 50,000 miles in 1992. A standard of 0.4 g/mi is expected to be phased in between 1994 and 1998 and 0.2 g/mi between 2003 and 2008.[5] A more efficient method of NO_x reduction than the present catalytic methods is required to meet these upcoming emission standards.

1.2 EXISTING EMISSION REDUCTION METHODS

Stationary- and mobile-source emissions can be controlled by postcombustion techniques or by combustion modification processes. Postcombustion methods involve the reduction of pollutants directly from the exhaust gas, while combustion modification is based on altering the chemical and thermal conditions under which air/fuel reactions occur to create NO_x. Catalytic reduction is a postcombustion technique that has been implemented on stationary sources. Selective catalytic reduction involves the reduction of NO_x in the presence of ammonia (NH_3) and a catalyst to produce nitrogen and water (H_2O).[3,4] Absorption-oxidation processes absorb the NO_x into a solution containing an oxidant, which converts the NO_x into a nitrate salt.[3]

Similar exhaust after-treatment methods that are currently used on automobiles are the three-way catalyst and the dual catalyst methods. In the three-way catalyst method, NO_x, hydrocarbons (HC), and carbon monoxide (CO) are simultaneously removed by using a reduction catalyst and adding air to the exhaust in a closed-loop system. The reducing catalyst is usually a metal oxide that is part of the iron group. In the dual catalyst method, a three-way catalyst is used in series with an oxidizing catalyst. The oxidizing catalyst can be a part of either group I, V, VI, or VIII of the periodic table.[6] Because most catalytic-reduction reactions require an inlet air temperature of 220-350°C to reach their maximum reduction capability, they do not work well under cold running conditions.

Many combustion modification techniques for reducing NO_x are currently in use with stationary sources. For example, flue gas recirculation reduces the combustion temperature and available oxygen by recirculating the relatively cool combustion gases from the stack.[2-4]

Staged combustion reduces the amount of oxygen available while lowering the peak operating temperature by introducing less air than necessary for complete combustion at each stage in a multiple burner system.[2,4]

Engine combustion modification techniques such as lean fuel/air ratio, stratified charge, and exhaust gas recirculation are used on mobile sources. A lean-burn technique has been used to simultaneously control the amounts of NO_x, CO, and HC. As the fuel/air equivalence ratio is reduced to 0.9, CO and HC emissions drop but NO_x emissions increase, because of higher combustion temperatures. An extremely lean mixture (0.8 fuel/air equivalence ratio) results in control of HC, CO, and NO_x, but the spark energy necessary to ignite the lean mixture is at least two orders of magnitude greater than what is used to ignite a rich mixture.[7] The stratified charge technique allows a rich fuel mixture into a small chamber containing the spark plug and a much leaner mixture into the main chamber to reduce the required combustion temperature. Exhaust gas recirculation (EGR), similar to that used in stationary sources, is also used in engines. By recirculating the exhaust gas, the postflame gas temperature is reduced, resulting in a reduction in thermal NO_x production.

These methods can be used to meet present emissions standards, but they are not adequate to reach the proposed standards because there are limits to their effectiveness for mobile sources. For example, catalytic reduction methods do not work well under cold conditions, and engine modification techniques may reduce the fuel economy of the car. A cost-effective method that can reduce emissions at any temperature and not affect the gas mileage of the car is needed.

1.3 MONOTOMIC NITROGEN METHOD

Recently, engineers have been developing a membrane for automotive application that separates the air stream into oxygen and nitrogen components. The oxygen-enriched stream is fed to the engine combustion chamber, while the nitrogen-enriched air is exhausted. The membrane can reach an efficiency of 99.9% N_2, but only when the pressure of the inlet air is raised to 100 psi. The advantages of an increase of oxygen to the combustion process are a reduction of HC and CO and improved fuel economy of the motor.[8] However, the concentration of NO_x in the exhaust increases.

This paper reports on research at Argonne National Laboratory (ANL) of a method that uses the nitrogen-enriched stream of the membrane to reduce NO and NO_x. The mechanism involves energizing the nitrogen with an electric arc to form monatomic nitrogen (N*). It is well known that N* atoms generated by the arc can reduce nitric oxide (NO) emissions by reversing the Zel'dovich step:[9]

$$N^* + NO \rightarrow N_2 + O \qquad (1)$$

This project examines the applicability of using N^* to reduce both NO and NO_2. The advantages of using this technology are that it can be low cost, works readily under cold-start

conditions, and will likely improve the fuel economy of an automobile. This control technology will permit the engine to burn leaner and more efficiently, meet future emission standards, and not rely on the current three-way catalytic converter (which requires the engine to run near stoichiometric continuously).

2 EXPERIMENTAL APPARATUS AND PROCEDURE

2.1 HIGH-VOLTAGE PULSER SYSTEM AND REACTION CHAMBER

Figure 2.1 presents a schematic diagram of the experimental setup. The system is used to determine the feasibility of employing an electric arc to create N* for reducing NO_x to nitrogen and oxygen. For these laboratory tests, a 50-kV charge from a power supply is used in conjunction with a pulser to create an electric arc. The pulser, manufactured for ANL by Ion Physics Corporation, consists of a series of capacitors and resistors enclosed in a cylindrical aluminum tank. The 50-kV charge from the power supply travels to the pulser through two external resistors. Once the charge reaches the pulser, it is stored in the system's capacitors until the pulser receives a signal from the trigger to release the charge. The frequency of the trigger can be altered during an experiment to vary the pulse of the electric arc. The high-voltage pulse from the pulser is delivered to a needle in the reaction chamber through a 1/4-in.-diameter metal tube insulated by Teflon. The electric arc then propagates from the needle to a ground electrode. A narrow, rounded tip on the ground electrode helps to reduce the motion of the arc and to keep it centered along the nitrogen gas stream. The metal tube provides a current path for the pulser to the reaction chamber, while simultaneously allowing for introduction of a pure nitrogen gas to the needle, forming a gas jet. The gas jet impinges on the ground electrode placed right in front of it.

The reaction chamber that houses the needle and ground electrode is a metal rectangular box that has a cross section measuring 4 in. × 4 in. and 4 ft long. The chamber is fitted with two windows, mounted on opposite sides, to allow observation of the arc, needle, and ground electrode characteristics. The needle is centered in and surrounded by a removable glass tube. The ground electrode is aligned with the needle center at a distance of 0.75 in. from the needle end. The gas stream is fed from the gas cylinders into the glass tube, which keeps the gas in close proximity to the arc, as pictured in Figure 2.2. The glass tube defines the cross-sectional flow area of the NO_x gas stream. The gas stream and the pure nitrogen jet always flow in the same direction. Three different diameters of glass tube were used to investigate the effects of confining the gas stream at various distances from the arc and assess the effects of different exhaust gas velocities on the NO_x reduction efficiency. Perpendicular to the end of the glass tube is a sample probe, consisting of an 1/8-in.-outside-diameter ceramic tube connected to Teflon tubing. The probe collects a representative gas sample that is pumped to the NO/NO_x and oxygen analyzers.

2.2 NO/NO_X AND OXYGEN ANALYZERS AND DATA ACQUISITION

A Beckman Model 951A NO/NO_x analyzer is used to monitor the NO and NO_x concentrations of the gas exiting the glass tube. The analyzer has two settings for measuring the exhaust. NO is directly measured by using the chemiluminescent method, and NO_x is measured by first converting NO_2 to NO and then using the chemiluminescent method for detection. Therefore, the analyzer measures only NO and the combination of NO_2 and NO

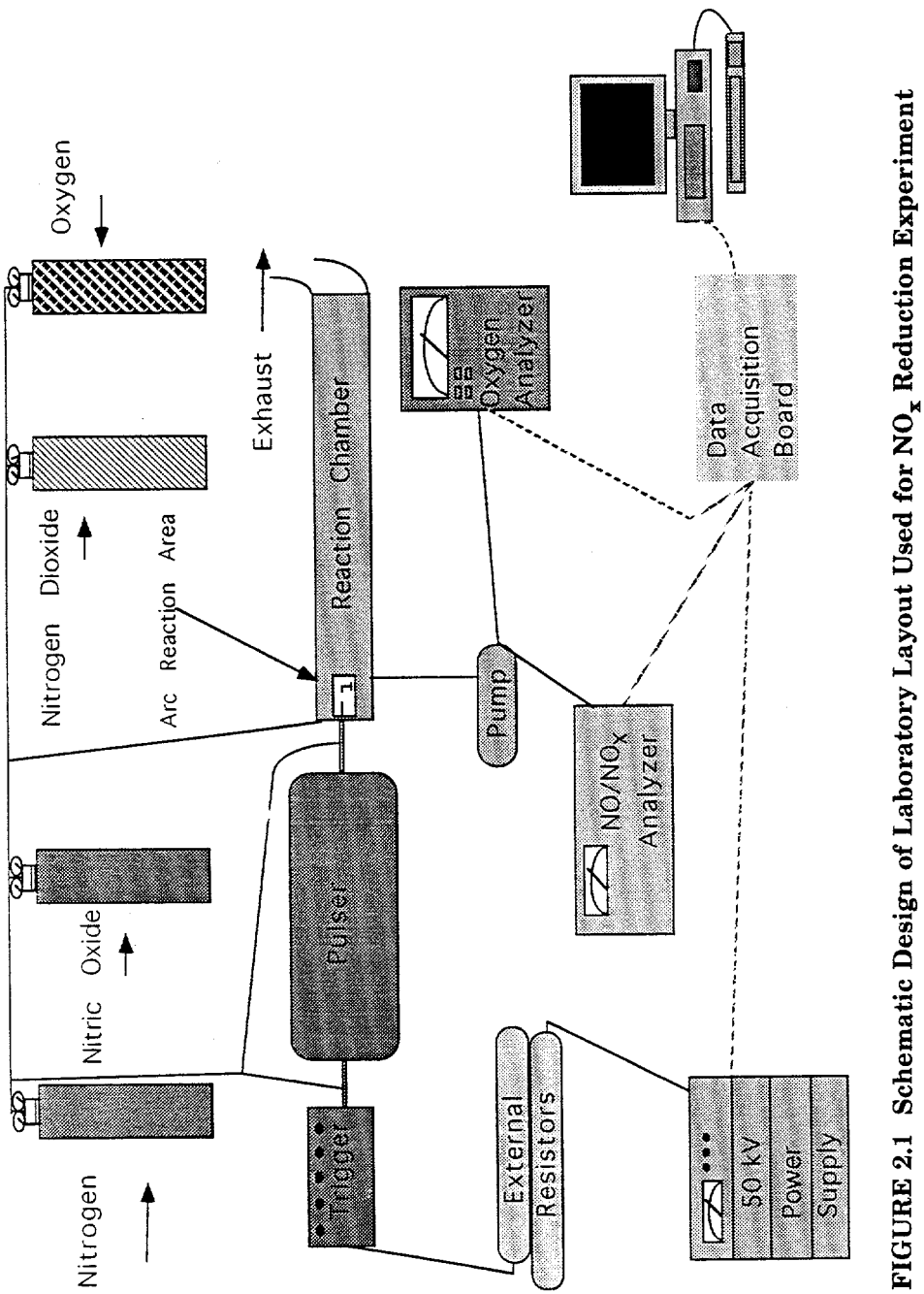

FIGURE 2.1 Schematic Design of Laboratory Layout Used for NO_x Reduction Experiment

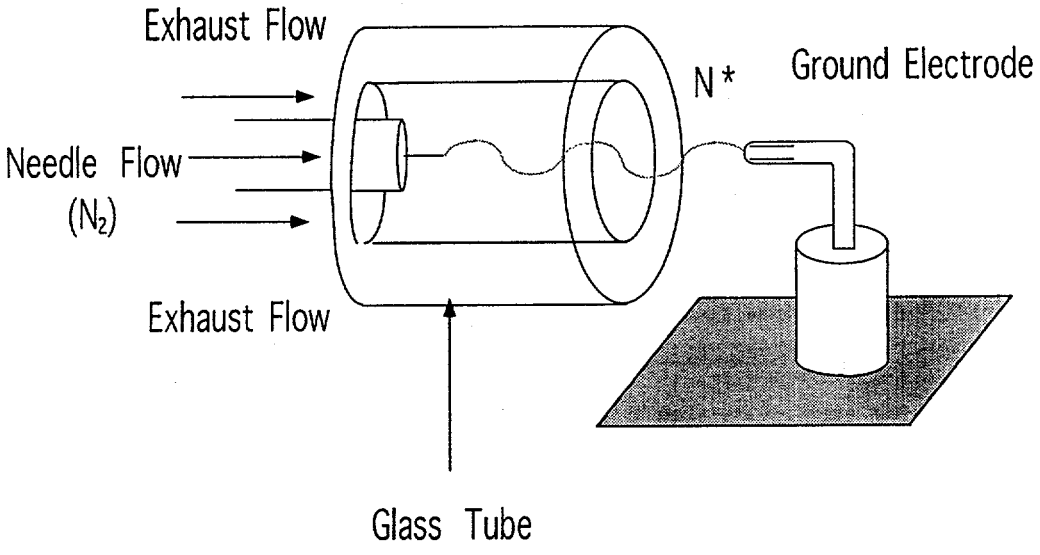

FIGURE 2.2 Arc Reaction Area Closeup

as NO_x. This analyzer is used to measure the initial concentrations of NO and NO_x before the arc is turned on, and to measure the amount of NO and NO_x left after the gas stream has reacted with the nitrogen ions produced by the arc. These two measurements are used to determine the reduction efficiencies of NO and NO_x for each set of experimental variables:

$$\text{NO Reduction Efficiency} = \frac{[NO]_{\text{before arc}} - [NO]_{\text{after arc}}}{[NO]_{\text{before arc}}} \quad \text{and} \tag{2}$$

$$NO_x \text{ Reduction Efficiency} = \frac{[NO_x]_{\text{before arc}} - [NO_x]_{\text{after arc}}}{[NO_x]_{\text{before arc}}} \tag{3}$$

In order to quantify the oxygen produced by the NO_x reduction with the pulsed electric arc, a sample from the gas stream is fed to an oxygen analyzer before and after the arc treatment. A Type A-Plus Oxygen Analyzer, manufactured by Delta F Corporation, with an in-line external gas scrubber, is used to measure the oxygen concentration in the sample. The scrubber contains small spheres of potassium permanganate to remove the NO/NO_2 gas that would otherwise interfere with the oxygen measurement. The oxygen analyzer uses a non-depleting sensor and operates on a simple coulometric process in which oxygen in the sample gas is reduced in an electrochemical cell. The sample gas diffuses through a barrier

to the cathode that is in contact with electrolyte solution; oxygen is reduced at this electrode to a hydroxyl (OH) ion:

$$O_2 + 2H_2O + 4e^- \rightarrow 4OH^- \quad \text{(cathode reaction)} \tag{4}$$

Assisted by potassium hydroxide electrolyte, the ions migrate to the anode, where they are oxidized back to oxygen:

$$4OH^- \rightarrow O_2 + 2H_2O + 4e^- \quad \text{(anode reaction)} \tag{5}$$

An external electromotive force (EMF) of 1.3 V dc drives the reaction in the sensor; the resulting cell current is directly proportional to the oxygen concentration in the gas stream. This current is measured using solid-state circuitry. The oxygen analyzer is capable of measuring oxygen levels from 10 ppm to 5%.

Data on the levels of NO, NO_x, and oxygen in the treated gas stream, as well as power supply current and voltage information, are transmitted to the data acquisition system in voltage signals. Data points are averaged over a 5- or 10-second time period and recorded in the computer buffer. Upon completion of the experiment, the data in the buffer are saved to the hard drive of a computer in a Microsoft Excel file.

2.3 EXPERIMENTAL PROCEDURE

Prior to each daily set of experiments, the oxygen analyzer is purged with pure nitrogen to remove residual oxygen in the connecting tubing and electrolytic cell. The NO/NO_x analyzer is turned on at least 45 min prior to the experiment to allow the converter to reach operating temperature. Next, the desired gas flows from each of the component gases are initiated and set with a Tylan flowmeter, so the majority of the oxygen in the reaction chamber is purged. A slight buildup of pressure in the reaction chamber is required to keep the outside oxygen from entering the reaction chamber through the exhaust tubing. The pump for transferring gas samples from the sample probe to the analyzers is activated, but the valve to the oxygen analyzer is not opened until approximately 5 min after the gas flow to the reaction chamber has started. This delay is to keep the oxygen from the reaction chamber out of the analyzer.

When the analyzers have stabilized, approximately 5-10 min after the sample has flowed through the oxygen analyzer, automated data acquisition is initiated. During the experiment, data such as the pulser frequency, gas flow, and instrument scale setting are recorded manually.

3 RESULTS

3.1 EXPERIMENTS WITH NO

In the first series of tests to determine the feasibility of using monatomic nitrogen to reduce NO_x, researchers simply used NO and N_2 for the gas stream and pure N_2 for the needle flow. Nitric oxide was selected as the initial exhaust gas because it is the most dominant nitrogen oxide in engine exhaust. The initial laboratory setup allowed investigation of the reactions among nitrogen, N*, and NO with different levels of electric arc power, gas stream and needle gas flows, and glass tube sizes.

By modifying the voltage and pulse frequency of the arc, the power output of the arc can be changed. As power to the arc is increased, a logarithmic increase ($1-e^x$) of NO reduction efficiency is observed. Figure 3.1 shows the reduction efficiency of NO from the gas stream as a function of the power for 450-ppm NO gas at a flow rate of 7.5 standard liters per minute (slpm) and a glass tube diameter of 17.5 mm. NO and NO_x reductions of 65% and 63%, respectively, were observed at 350 W. The difference in reduction efficiency for the NO and the NO_x is caused by statistical error. In general, the maximum reductions in NO and NO_x were always obtained at the maximum power supply setting (approximately 350 W).

The flow rate of the nitrogen through the needle was varied to test the effect on NO reduction at a constant arc power. As shown in Figure 3.2, the change in flow rate of nitrogen through the needle, at a constant gas stream flow and with a glass tube diameter of 17.5 mm, did not change the reduction efficiency for 450-ppm NO. The reduction efficiency remains within ±5% for needle flows of 0 to 1.28 slpm and a constant gas stream flow rate of 7.5, 15, or 20 slpm. This effect may be caused by the low flow rates of nitrogen through the needle compared to the total gas flow.

Tests were also conducted to determine the effect of varying the gas stream cross-sectional flow area around the arc while keeping the power constant. Glass tubes measuring 12, 17.5, and 19 mm in diameter were tested using the same gas stream. As indicated in Figures 3.3 and 3.4, the results of the experiment with 450-ppm NO and an arc power of 350 W were not conclusive, but the reduction efficiency seems to improve with smaller flow areas. The smaller-diameter glass tubes may be more effective than the larger-diameter (19 mm) tube, because the smaller tube keeps the NO closer to the N*. However, when the 12-mm-diameter tube was used, the arc migrated to the wall of the surrounding glass tube rather than traveling to the ground electrode. Figure 3.5 shows the decrease in NO reduction efficiency when the arc comes in contact with the wall. The reduction efficiency when the 17.5-mm-diameter glass tube was used (no arc-glass contact) was significantly higher than the efficiency when the 12-mm cylinder was in place (arc-wall contact). The arc was not centered in the nitrogen stream when it contacted the glass, so the nitrogen stream was not as completely energized. The best reduction results were obtained with the 17.5-mm-diameter glass tube, so it was used most in the experiments.

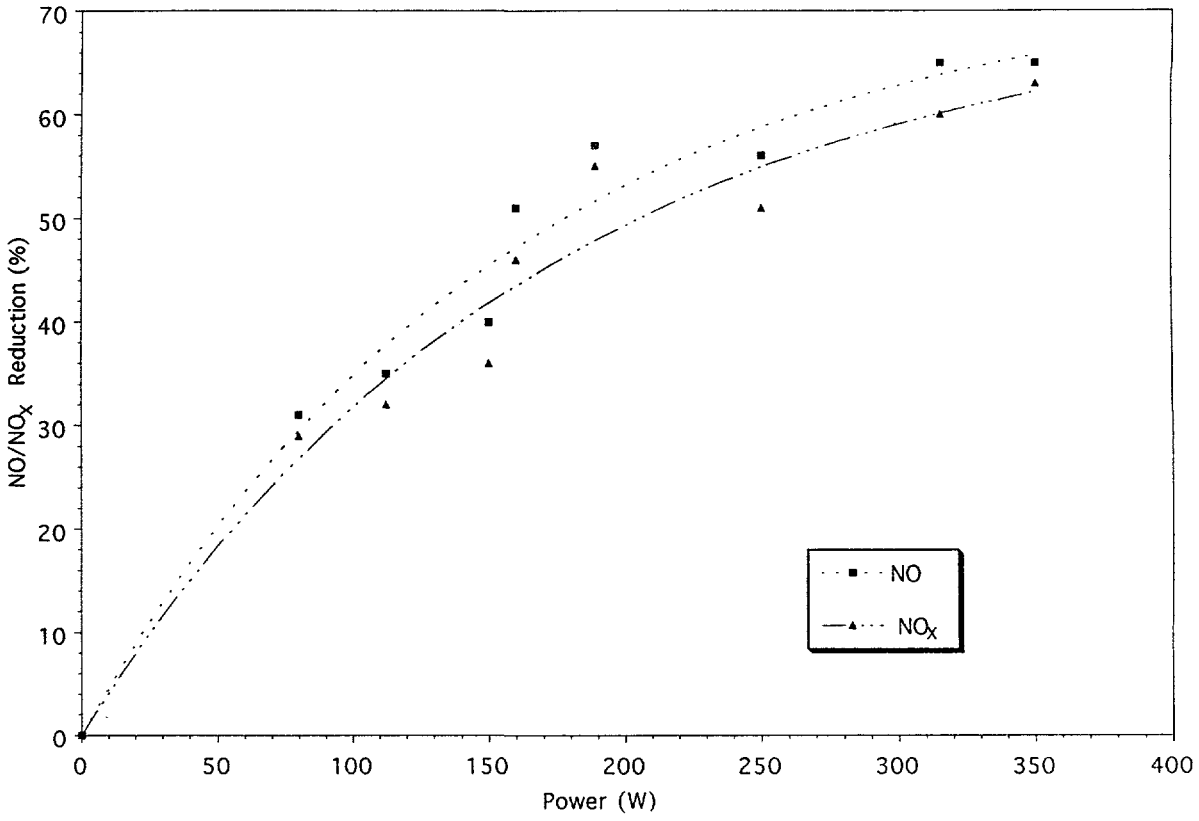

FIGURE 3.1 NO and NO_x Reduction Efficiency vs. Power (for 450 ppm NO, gas flow of 7.5 slpm, and glass tube diameter of 17.5 mm)

The effect of the gas stream velocity on NO/NO_x reduction efficiency was studied next. The velocity was determined by dividing the gas stream volumetric flow by the cross-sectional area of the glass tube around the arc. These tests demonstrated that, for the same cross-sectional area, lower gas velocities improved the reduction efficiency of NO and NO_x. Figure 3.6 shows a linear relationship between the increase in velocity and the decrease in reduction efficiency for the same glass tube diameter at 50 kV and 60 Hz. This linear relationship occurs because a unit volume of gas stream comes in contact with more N* at these lower velocities. Because N* is formed by the arc, the amount of N* present in the glass tube is a function of the arc power, which in turn is a function of the power supply voltage and pulser frequency. If the velocity of the exhaust gas is high, a unit volume of gas may pass through the tube during only one pulse; if the velocity is low, the unit volume may pass through during two or more pulses.

Different concentrations of NO in the nitrogen gas stream were also tested, and the results are shown in Figure 3.7. A tenfold increase in NO concentration caused a decrease in the NO_x reduction efficiency by about a third. The low reduction efficiency at the higher

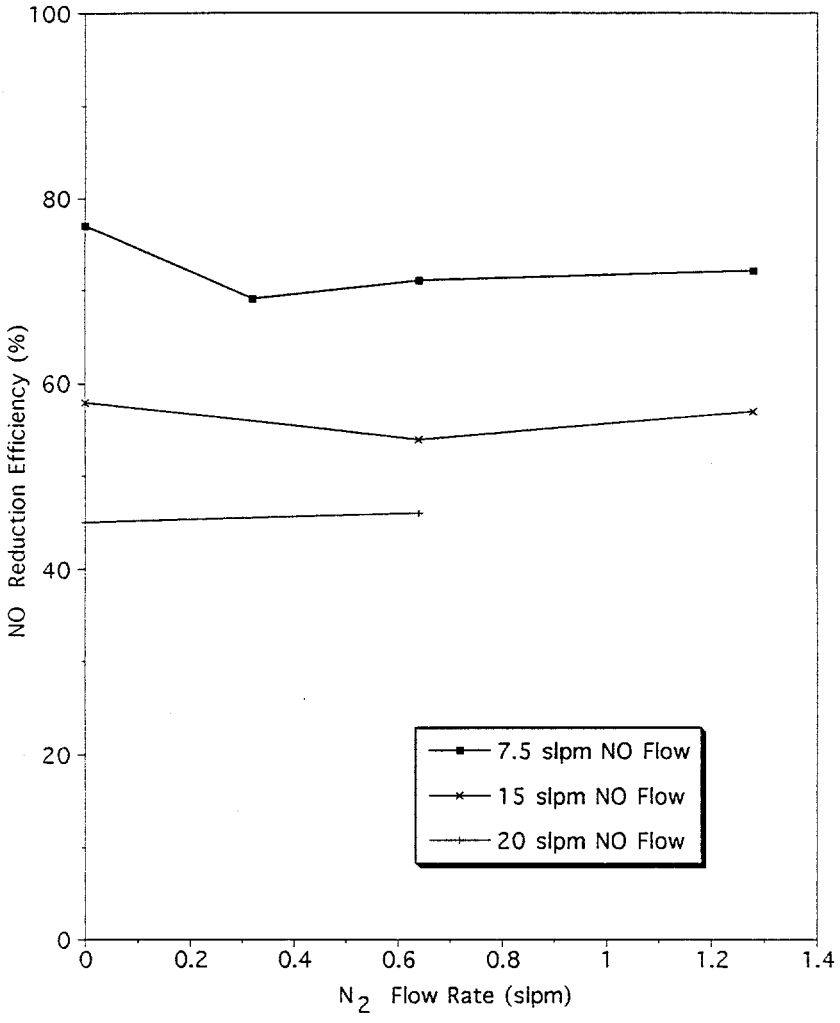

FIGURE 3.2 NO Reduction Efficiency vs. Needle Flow Rate (for 450 ppm NO and glass tube diameter of 17.5 mm)

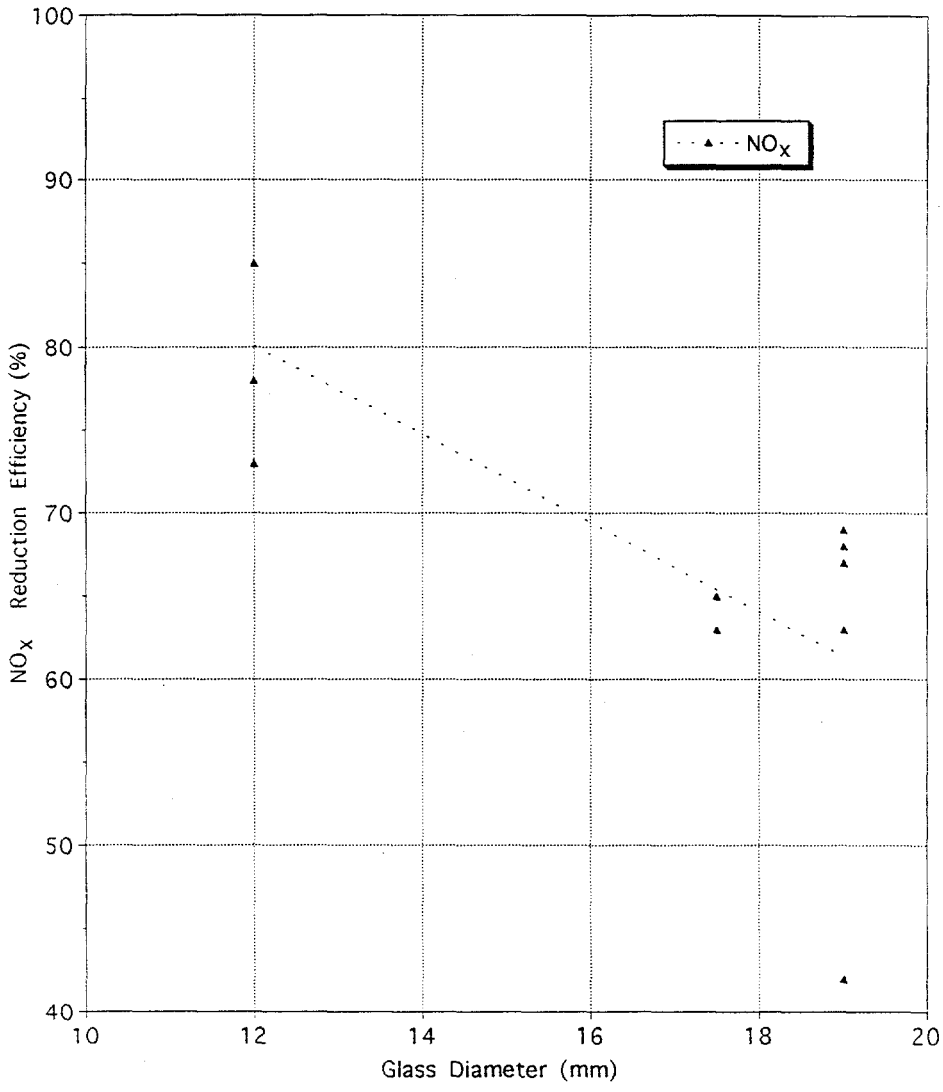

FIGURE 3.3 NO_x Reduction Efficiency vs. Flow Diameter (for 450 ppm NO, gas flow of 7.5 slpm, and power of approximately 350 W)

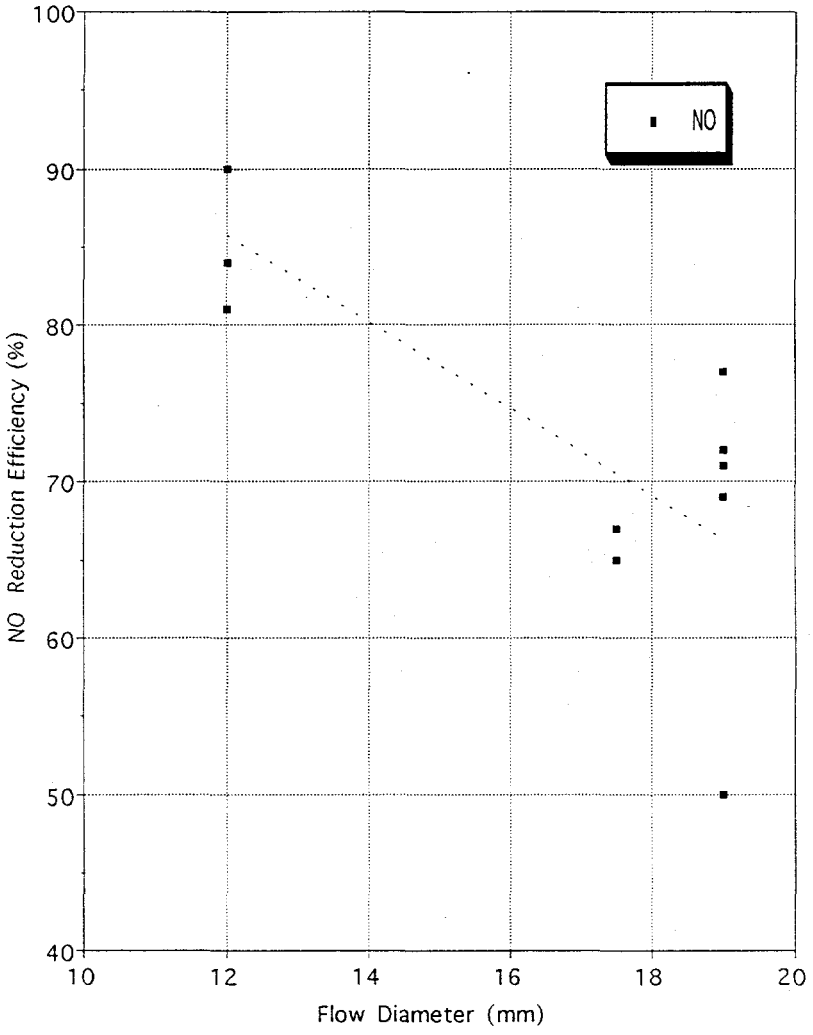

FIGURE 3.4 NO Reduction Efficiency vs. Flow Diameter (for 450 ppm NO, gas flow of 7.5 slpm, and power of approximately 350 W)

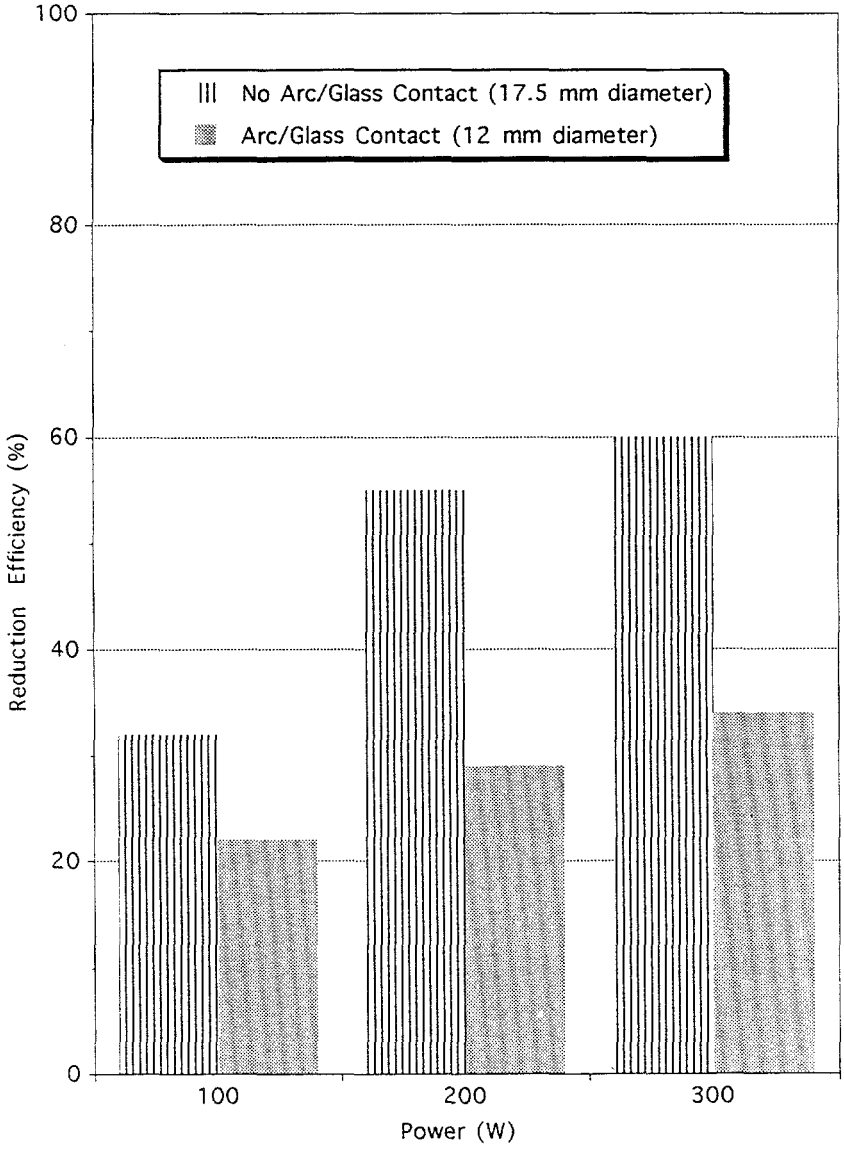

FIGURE 3.5 Reduction Efficiency by Arc/Glass Contact Compared to Efficiency at Larger Glass Tube Diameter

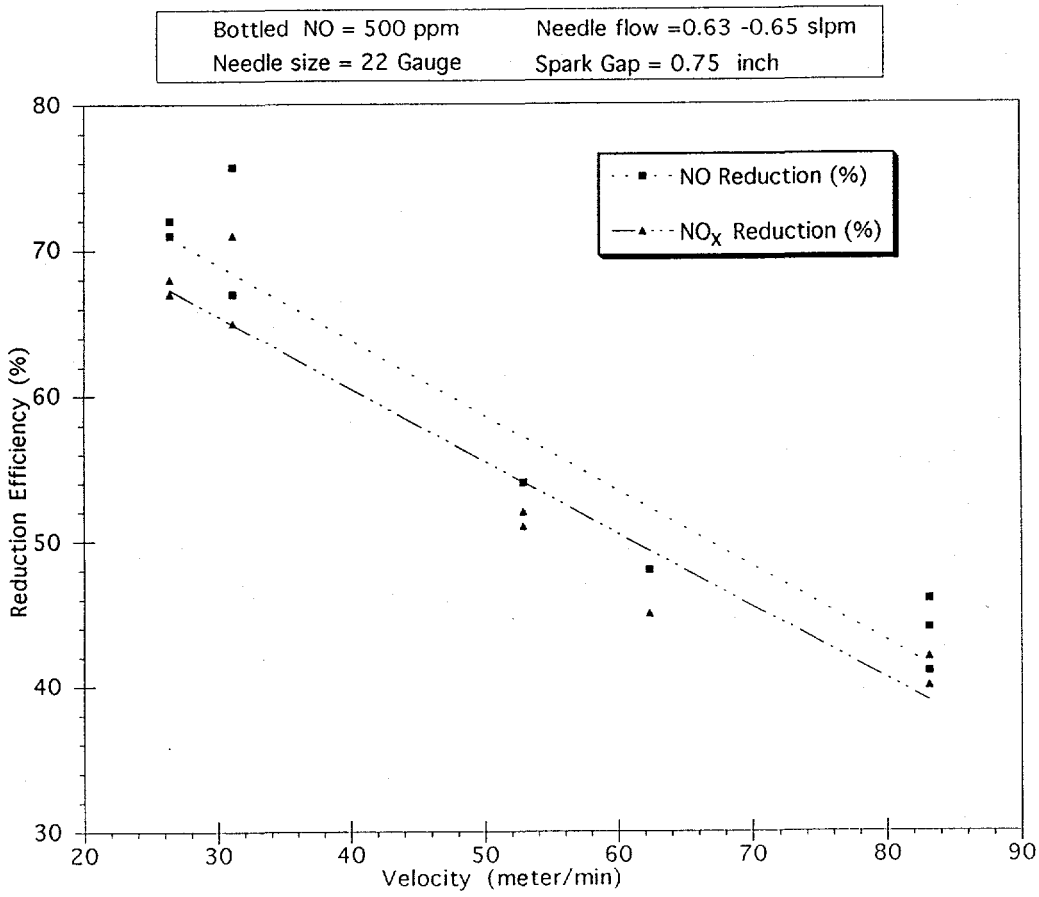

FIGURE 3.6 Velocity vs. NO and NO_x Reduction Efficiency (for inside glass tube diameters of 19 mm and 17.5 mm at 50 kV and 60 Hz)

concentration could be improved by increasing the needle nitrogen flow and/or the electric arc power (unfortunately, power could not be further increased with the present experimental setup).

3.2 EXPERIMENTS WITH NO_2 AND NO/NO_2 MIXTURES

Initial tests were conducted using only NO_2 and pure nitrogen in the gas stream. As in the previous tests, the reduction efficiency was measured as a function of arc power. Figure 3.8 shows the concentration of NO_x in the gas stream with an increase in arc power. In this test, the initial concentration was 225 ppm NO_2, the flow rate was 7.5 slpm, and the

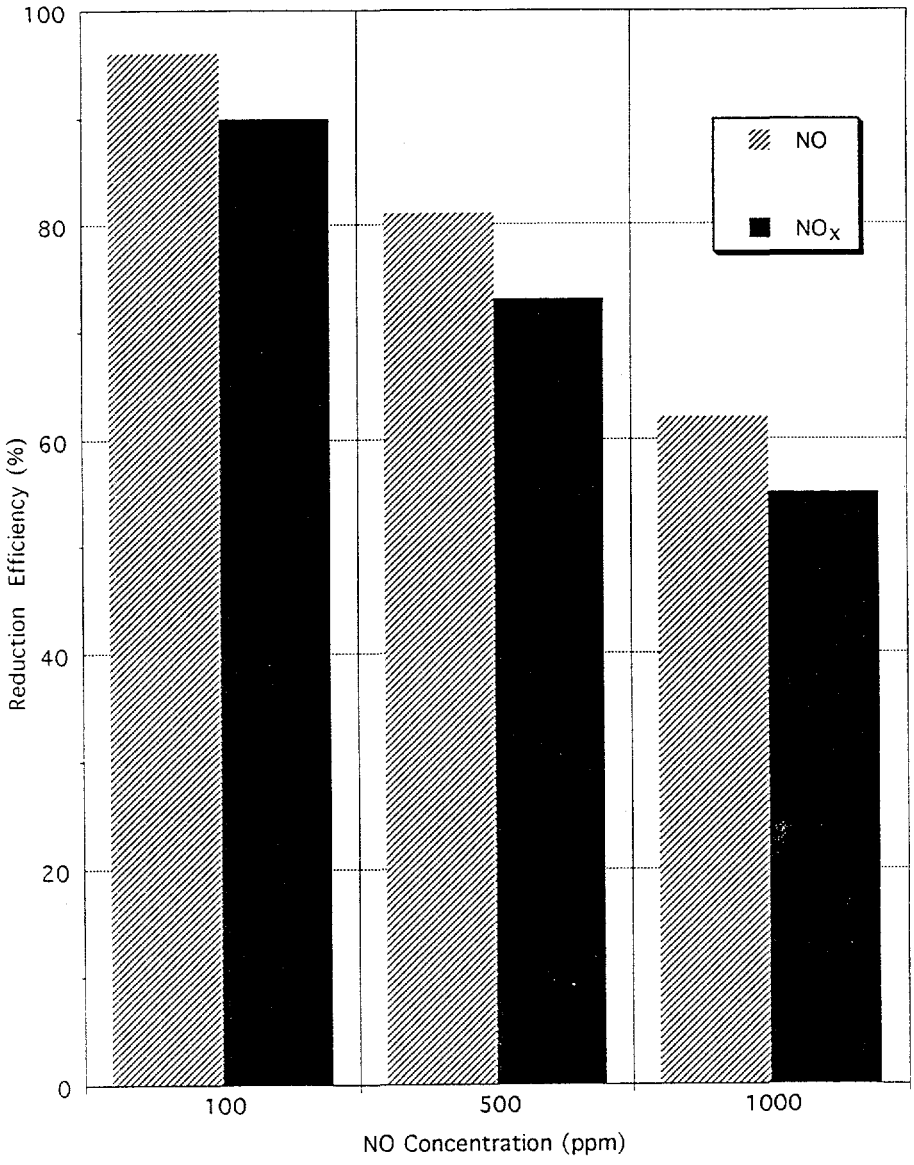

FIGURE 3.7 Reduction Efficiency vs. NO Gas Concentration (at gas flow of 7.5 slpm, power of approximately 350 W, and glass tube diameter of 12 mm)

glass tube diameter was 17.5 mm. The reduction of NO_2 was accompanied by a slight increase in NO that was created through the following competing reaction:

$$N^* + NO_2 \rightarrow 2\ NO \qquad (6)$$

Although NO was created during the breakdown of NO_2, the overall NO_x reduction was still 65%. These results are comparable to the results obtained using NO mixtures.

Tests were then conducted with nitrogen gas streams containing 450 ppm NO and 225 ppm NO_2 to evaluate the effects of gas stream flow rates on NO/NO_x reduction efficiency. For this test, the power was maintained at 350 W. Figures 3.9 and 3.10 show that the rate at which the gas stream flows over the arc has a significant effect on the reduction efficiencies. NO and NO_2 removal efficiencies decrease with increased flow rates. As the flow rate increases, the NO_x molecules pass more quickly through the arc reaction area with N*.

Different concentrations of NO_2 in the nitrogen gas stream were tested. As shown in Figure 3.11, the NO_x reduction efficiency decreased from 84% to 65% with the fivefold increase of NO_2 concentration in the gas stream at a power of 350 W. This decrease in reduction efficiency is similar to the decrease observed in the NO tests (Figure 3.7). The decrease in reduction efficiency with an increase in concentration of NO_x may be caused by a limit on the number of NO_x molecules with which a unit volume of N* can react in a given period of time.

In the NO/NO_2 mixture tests, the concentration of NO was kept constant at 750 ppm, while the concentration of NO_2 was varied to maintain fixed NO/NO_2 concentration ratios. The results from these tests are graphed in Figure 3.12. Although the results are scattered, they do indicate that the reduction efficiencies of NO, NO_2, and NO_x increase with electric arc power. The reductions of NO were higher when the ratio of NO to NO_2 was higher (20:1 vs. 10:1). However, this trend was reversed for the NO_2 reductions. Consequently, the overall NO_x reduction efficiencies were very similar for the two different gas mixtures.

3.3 OXYGEN TESTS

Several tests were conducted to determine the effect of oxygen on NO_x reduction efficiency. Different quantities of oxygen were used in the needle flow and in the gas stream flow. The total oxygen content varied from 0.5% to 9.6% of the total gas flow for these tests.

Figure 3.13 shows that both NO and NO_x reduction efficiencies decrease with increasing oxygen content in the gas stream. The decrease was rapid from 0% to 2% oxygen, but ceased at around 4% oxygen. It seems that some sort of equilibrium was reached for the N_2, O_2, NO, and NO_2 system. Figure 3.14 demonstrates that oxygen has a similar effect on reduction whether the oxygen is in the gas stream or in the needle flow.

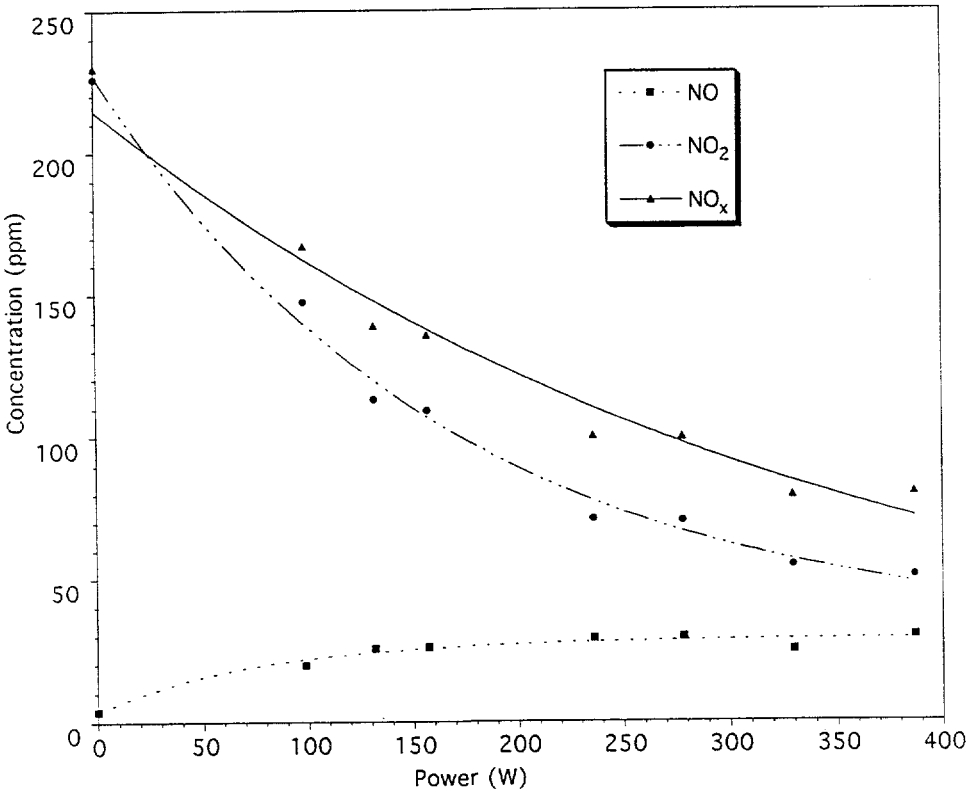

FIGURE 3.8 NO_x Concentration vs. Power (for 225 ppm NO_2, gas flow of 7.5 slpm, and glass tube diameter of 17.5 mm)

This decrease in reduction efficiency is probably caused by the monatomic oxygen (O*) induced by the pulsed arc. The O* reacts with N* and NO to form NO and NO_2. During tests with an oxygen content of 5% or more of the total flow, more NO_2 was created than was reduced.

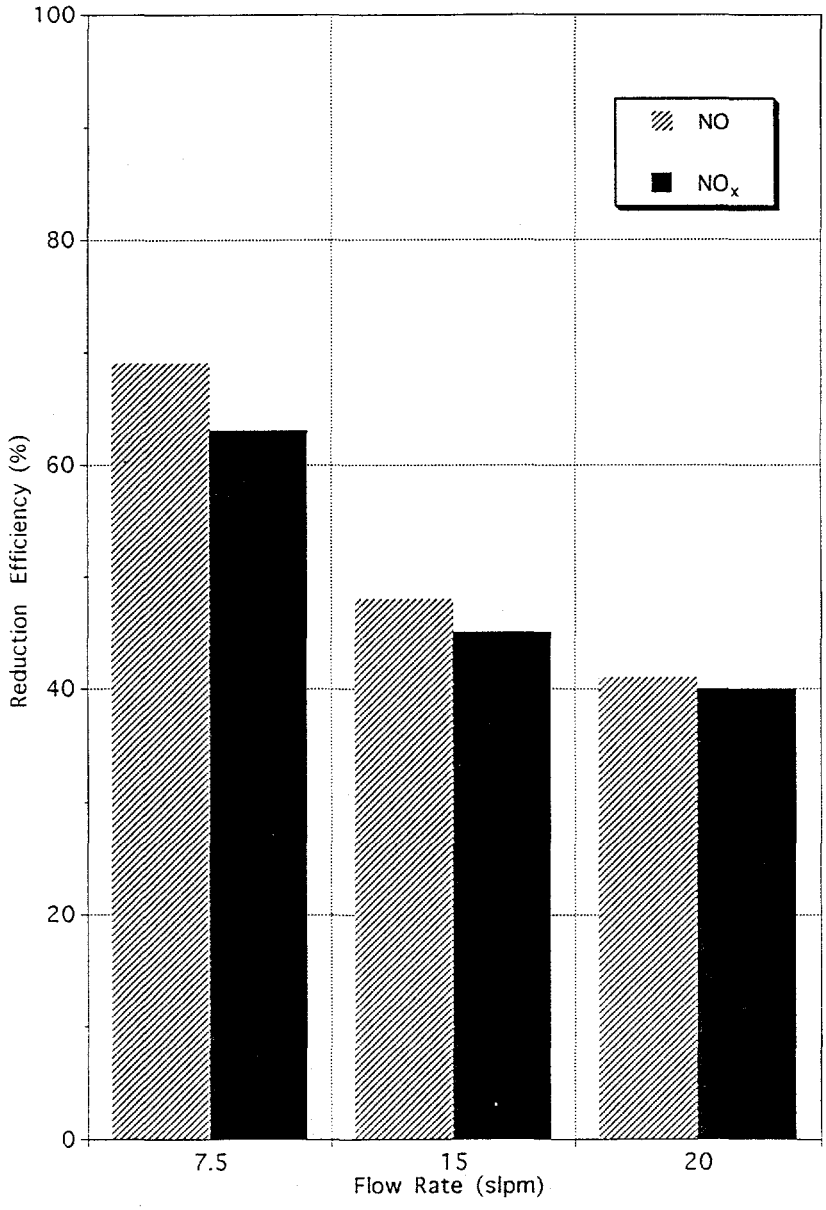

FIGURE 3.9 NO Reduction Efficiency vs. Flow Rate (for 450 ppm NO, gas flow of approximately 350 W, and glass tube diameter of 17.5 mm)

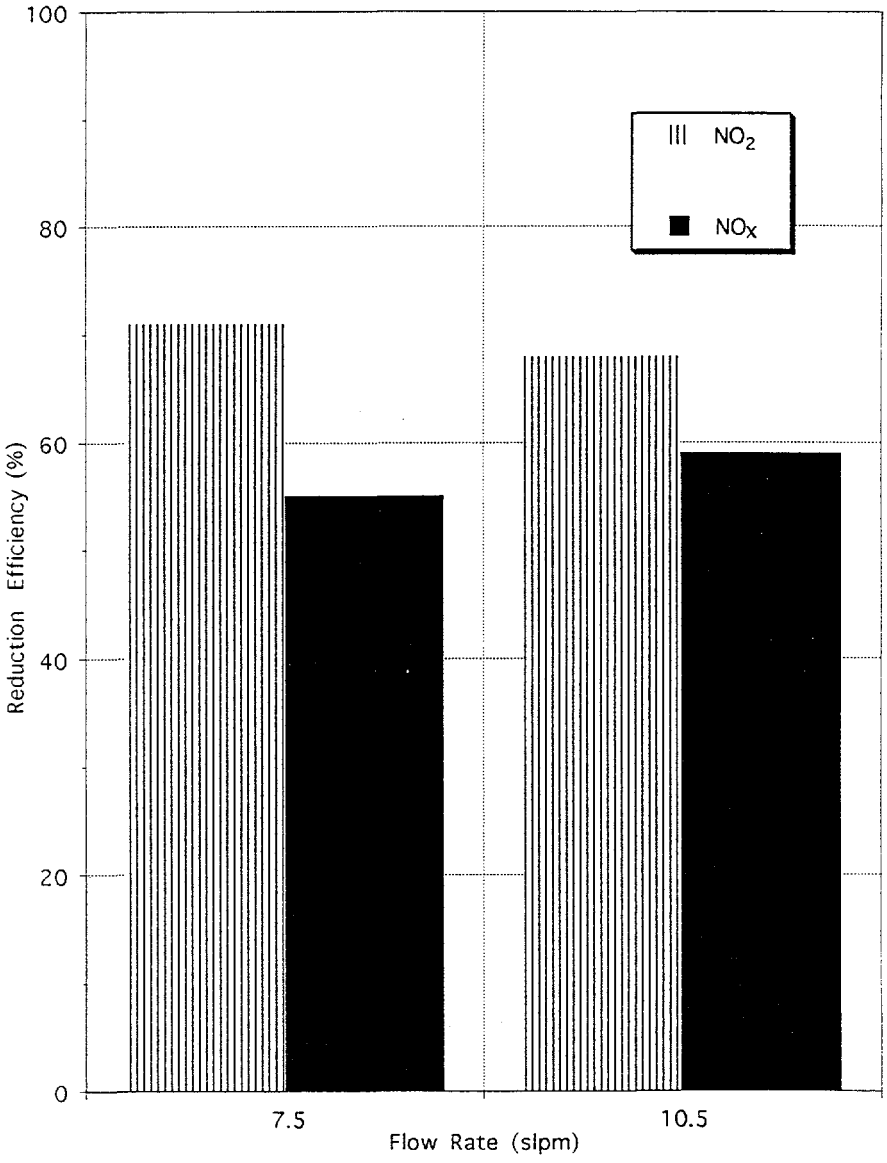

FIGURE 3.10 NO_2 Reduction Efficiency vs. Flow Rate (for 225 ppm NO_2, power of approximately 350 W, and glass tube diameter of 17.5 mm)

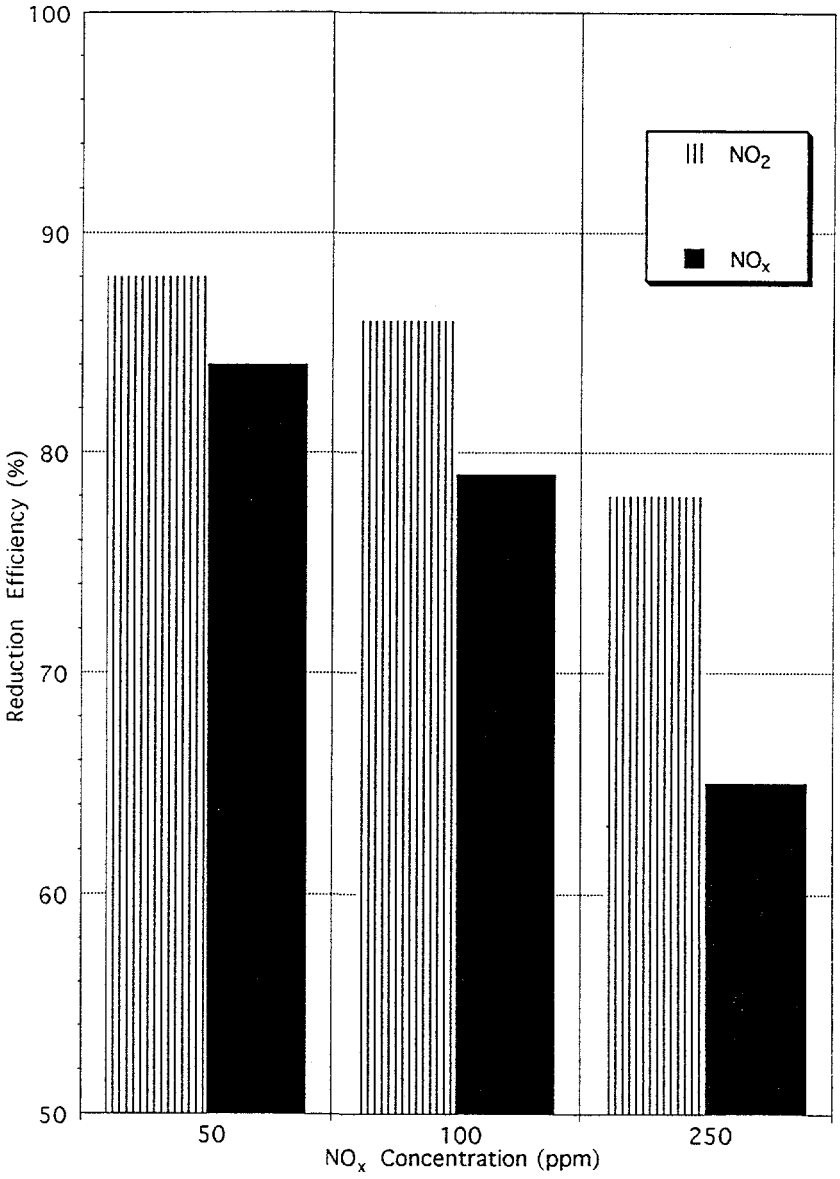

FIGURE 3.11 NO_2 Reduction Efficiency vs. NO_x Gas (at flow rate of 7.5 slpm power of approximately 350 W, and glass tube diameter of 17.5 mm)

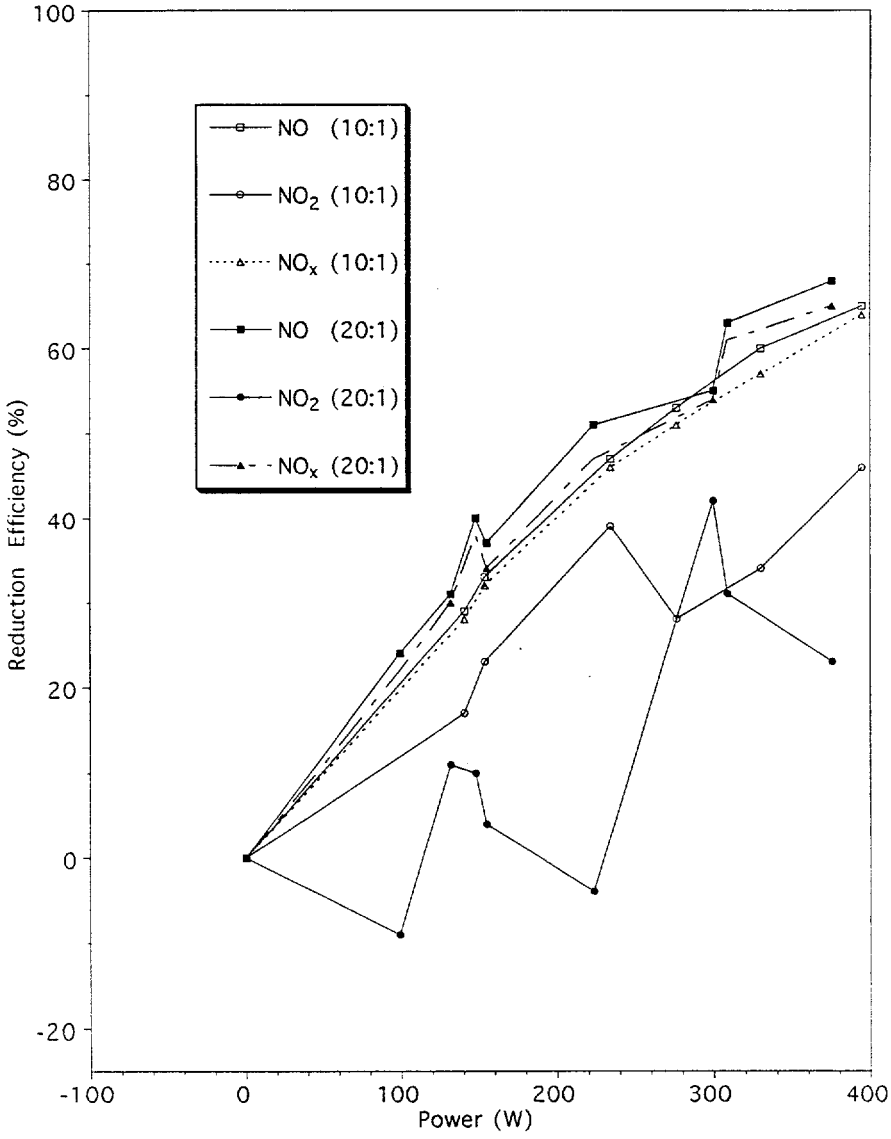

FIGURE 3.12 Reduction Efficiency vs. Power for Different NO-to-NO_2 Ratios (at flow rate of 7.5 slpm, initial NO concentration of 750 pm, and glass tube diameter of 17.5 mm)

Initial NO =500 ppm	Needle Size = 22 Gauge	Needle Flow = 0.65 slpm
Exhaust Flow = 7.5 slpm	Exhaust Diameter = 17.5 mm	Spark Gap = 0.75 in.

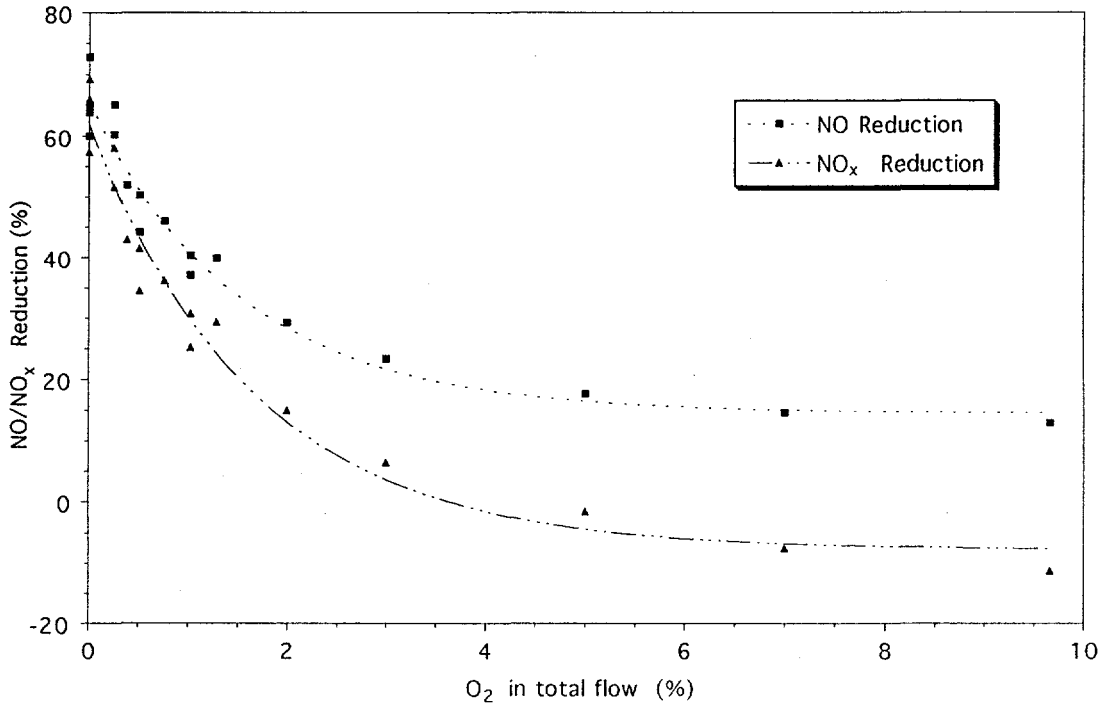

FIGURE 3.13 Percent Reduction of NO/NO_x vs. Percent Oxygen Present in the Gas Stream (at 45 kV and 60 Hz)

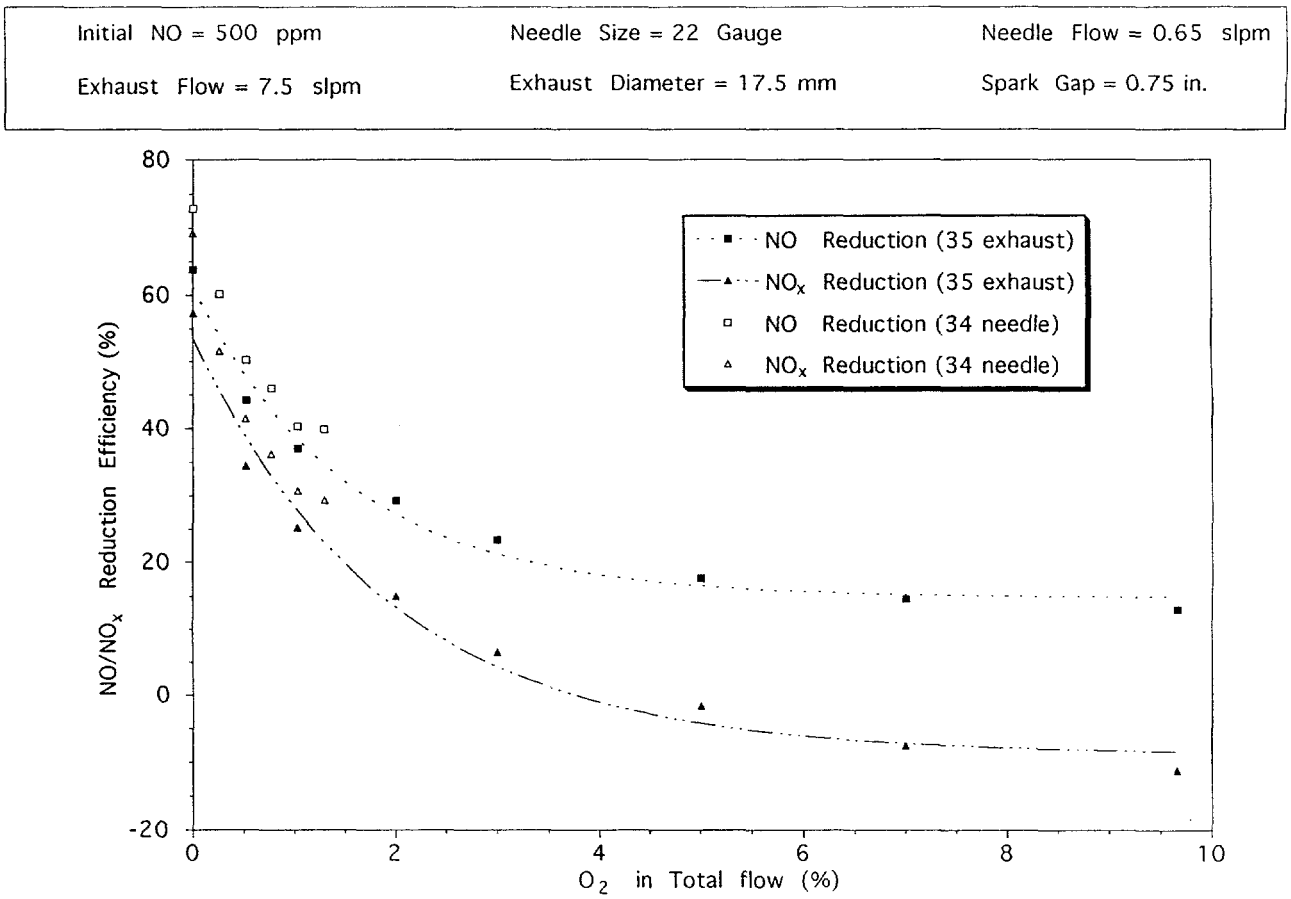

FIGURE 3.14 Reduction vs. Oxygen with O_2 Flow in the Needle or in the Exhaust (at 45 Kv and 60 Hz)

4 CONCLUSIONS AND RECOMMENDATIONS

The experiments conducted show how different variables affect the ability of monatomic nitrogen to reduce NO and NO_x. Increased reduction efficiency was observed with an increase in power and a decrease in the gas stream concentration, velocity, and flow rate. A decrease in the cross-sectional flow area of the gas stream (the glass tube diameter) improved reduction until the arc began contacting the glass wall. Overall, O_2 and NO_2 decreased NO and NO_x reduction, and even when O_2 and NO_2 were maintained at a small percentage of the total gas flow, significant reductions were still observed.

Further work is needed to reduce the deleterious effects of oxygen on NO/NO_x reduction efficiency. The reaction chamber should be modified to prevent the oxygen from being energized by the arc, and experiments using real engine exhaust should be performed to evaluate the merits of this technology for automotive applications.

5 REFERENCES

1. Freeman, G., C.M. Shy, D.E. Gardner, and R.G. Derwent, *Oxides of Nitrogen: Environmental Health Criteria 4*, World Health Organization, Geneva (1977).

2. Hall, R.E. and J.S. Bowen, Jr., "State-of-the-Art Combustion Modification NO_x Control for Stationary Combustion Equipment," *Air Pollution by Nitrogen Oxides*, pp. 635-651 (1982).

3. Martin, A.E., *Emission Control Technology for Industrial Boilers*, Noyes Data Corporation, Park Ridge, New Jersey (1981).

4. Princiotta, F.T., "Stationary Source NO_x Control Technology Overview," *Air Pollution by Nitrogen Oxides*, pp. 737-745 (1982).

5. Carlos, T.V. and R. Currie, "California Clean Air Act — A Compliance Strategy for the City of San Diego's Emergency Fleet," City of San Diego (1992).

6. Lawrence, A.A. "Catalytic Conversion of Automobile Exhaust Gas Containing Nitrogen Oxide Impurities," *Nitrogen Oxides Emission Control*, pp. 137-145 (1972).

7. Bradow, R.L., "Nitrogen Oxide Emissions from Motor Vehicles," *Air Pollution by Nitrogen Oxides*, pp. 115-129 (1982).

8. Ng, H.K., R.R. Sekar, S.W. Kraft, and K.R. Stamper, *The Potential Benefits of Intake Air Oxygen Enrichment in Spark Ignition Engine Powered Vehicles*, SAE Paper 932803 (1993).

9. Hilliard, J.C. and F.J. Weinberg, "Effect of Nitrogen-Containing Plasmas on Stability, NO Formation and Sooting of Flames," *Nature*, Vol. 259, pp. 556-557 (February 19, 1976).

APPENDIX:

DATA

Table	Figure
A.1	3.1
A.2	3.2
A.3	3.3
A.4	3.4
A.5	3.5
A.6	3.6
A.7	3.7
A.8	3.8
A.9	3.9
A.10	3.10
A.11	3.11
A.12	3.12
A.13	3.13
A.14	3.14

TABLE A.1

	Power (W) Figure 3.1	NO Figure 3.1	NO_x Figure 3.1
0	0.0000	0.0000	0.0000
1	80.000	31.000	29.000
2	112.50	35.000	32.000
3	150.00	40.000	36.000
4	160.00	51.000	46.000
5	189.00	57.000	55.000
6	250.00	56.000	51.000
7	315.00	65.000	60.000
8	350.00	65.000	63.000

TABLE A.2

	Needle N_2 Flow Rate (slpm) Figure 3.2	7.5 slpm NO Flow Figure 3.2	15 slpm NO Flow Figure 3.2	20 slpm NO Flow Figure 3.2
0	0.0000	77.000	58.000	45.000
1	0.32000	69.000		
2	0.64000	71.000	54.000	46.000
3	1.2800	72.000	57.000	

TABLE A.3

	Glass Diameter (mm) Figure 3.3	NO_x Reduction Figure 3.3
0	12.000	85.000
1	12.000	85.000
2	12.000	78.000
3	12.000	73.000
4	17.500	65.000
5	17.500	63.000
6	19.000	69.000
7	19.000	67.000
8	19.000	68.000
9	19.000	63.000
10	19.000	42.000

TABLE A.4

	Glass Diameter (mm) Figure 3.4	NO Reduction Efficiency Figure 3.4
0	12.000	90.000
1	12.000	90.000
2	12.000	84.000
3	12.000	81.000
4	17.500	67.000
5	17.500	65.000
6	19.000	77.000
7	19.000	72.000
8	19.000	71.000
9	19.000	69.000
10	19.000	50.000

TABLE A.5

	Power (W) Figure 3.5	No Arc/Glass Contact (17.5 mm) Figure 3.5	Arc/Glass Contact (12 mm) Figure 3.5
0	100.00	32.000	22.000
1	200.00	55.000	29.000
2	300.00	60.000	34.000

TABLE A.6

	Velocity Figure 3.6	NO Reduction (%) Figure 3.6	NO_x Reduction (%) Figure 3.6	Glass I.D.	I.D.* Velocity
0	52.9	54	51	19	0.79572
1	26.45	71	68	19	0.79572
2	26.45	72	67	19	0.50255
3	52.9	54	52	19	1.0051
4	52.9	54	51	19	0.50255
5	62.36	48	45	17.5	0.50255
6	31.18	67	65	17.5	1.0051
7	83.15	46	42	17.5	1.0051
8	83.15	44	41	17.5	1.0913
9	83.15	41	40	17.5	0.54565
10	31.18	75.7	71	17.5	1.4551
					1.4551
					1.4551
					0.54565

TABLE A.7

	NO Concentration (ppm) Figure 3.7	NO Figure 3.7	NO_x Figure 3.7
0	100.00	96.000	90.000
1	500.00	81.000	73.000
2	1000.0	62.000	55.000

TABLE A.8

	Power (W) Figure 3.8	NO Figure 3.8	NO_2 Figure 3.8	NO_x Figure 3.8
0	0.0000	3.9400	225.95	229.89
1	98.340	19.790	147.35	167.14
2	131.71	25.690	113.10	138.79
3	157.10	26.170	109.29	135.46
4	235.90	28.920	71.130	100.05
5	278.06	29.440	70.390	99.830
6	329.57	24.860	54.440	79.300
7	386.87	29.610	50.770	80.380

TABLE A.9

	NO Flow Rate (slpm) Figure 3.9	NO Figure 3.9	NO_x Figure 3.9
0	7.5000	69.000	63.000
1	15.000	48.000	45.000
2	20.000	41.000	40.000

TABLE A.10

	NO2 Flow Rate (slpm) Figure 3.10	NO_2 Figure 3.10	NO_x Figure 3.10
0	7.5000	71.000	55.000
1	10.500	68.000	59.000

TABLE A.11

	NO_x Concentration Figure 3.11	NO_2 Figure 3.11	NO_x Figure 3.11
0	50.000	88.000	84.000
1	100.00	86.000	79.000
2	250.00	78.000	65.000

TABLE A.12

	Power (W) Figure 3.12	NO (10:1) Figure 3.12	NO_2 (10:1) Figure 3.12	NO_x (10:1) Figure 3.12	NO (20:1) Figure 3.12	NO_2 (20:1) Figure 3.12	NO_x (20:1) Figure 3.12
0	0.0000	0.0000	0.0000	0.0000	0.0000	0.0000	0.0000
1	140.76	29.000	17.000	28.000			
2	153.96	33.000	23.000	32.000			
3	234.37	47.000	39.000	46.000			
4	276.73	53.000	28.000	51.000			
5	330.31	60.000	34.000	57.000			
6	394.67	65.000	46.000	64.000			
7	99.220				24.000	-9.0000	22.000
8	132.11				31.000	11.000	30.000
9	148.08				40.000	10.000	38.000
10	155.00				37.000	4.0000	34.000
11	223.58				51.000	-4.0000	47.000
12	300.00				55.000	42.000	54.000
13	309.31				63.000	31.000	61.000
14	375.66				68.000	23.000	65.000
15	0.0000						

TABLE A.13

	O_2 in Total Flow (%) Figure 3.13	NO Reduction Figure 3.13	NO_x Reduction Figure 3.13
0	0.52	44.21	34.49
1	1.03	37.06	25.22
2	2	29.31	14.99
3	3	23.41	6.44
4	5	17.67	-1.57
5	7	14.62	-7.57
6	9.66	12.91	-11.19
7	0.26	60.2	51.6
8	0.52	50.3	41.5
9	0.77	46	36.2
10	1.03	40.4	30.8
11	1.29	39.9	29.4
12	0	72.8	69.2
13	0	63.83	57.33
14	0	60	66
15	0	65	60
16	0.39	52	43
17	0.26	65	58

TABLE A.14

	O_2 Percent in Total Flow Figure 3.14	NO Reduction (35 exhaust) Figure 3.14	NO_x Reduction (35 exhaust) Figure 3.14	NO Reduction (34 needle) Figure 3.14	NO_x Reduction (34 needle) Figure 3.14
0	0.52	44.21	34.49		
1	1.03	37.06	25.22		
2	2	29.31	14.99		
3	3	23.41	6.44		
4	5	17.67	-1.57		
5	7	14.62	-7.57		
6	9.66	12.91	-11.19		
7	0.26			60.2	51.6
8	0.52			50.3	41.5
9	0.77			46	36.2
10	1.03			40.4	30.8
11	1.29			39.9	29.4
12	0			72.8	69.2
13	0	63.83	57.33		